



Article

A Framework for Survey Planning Using Portable Unmanned Aerial Vehicles (pUAVs) in Coastal Hydro-Environment

Ha Linh Trinh¹, Hieu Trung Kieu¹, Hui Ying Pak^{1,2}, Dawn Sok Cheng Pang¹, Angel Anisa Cokro¹ and Adrian Wing-Keung Law^{1,3,*}

¹ Environmental Process Modelling Centre, Nanyang Environment and Water Research Institute, Nanyang Technological University, Singapore 637141, Singapore; halinh.trinh@ntu.edu.sg (H.L.T.); trunghieu.kieu@ntu.edu.sg (H.T.K.); pakh0001@e.ntu.edu.sg (H.Y.P.); dawn.pang@ntu.edu.sg (D.S.C.P.); angelanisa.cokro@ntu.edu.sg (A.A.C.)

² Interdisciplinary Graduate Programme, Graduate College, Nanyang Technological University, Singapore 637141, Singapore

³ School of Civil and Environmental Engineering, Nanyang Technological University, Singapore 637141, Singapore

* Correspondence: cwklaw@ntu.edu.sg

Abstract: Recently, remote sensing using survey-grade UAVs has been gaining tremendous momentum in applications for the coastal hydro-environment. UAV-based remote sensing provides high spatial and temporal resolutions and flexible operational availability compared to other means, such as satellite imagery or point-based in situ measurements. As strict requirements and government regulations are imposed for every UAV survey, detailed survey planning is essential to ensure safe operations and seamless coordination with other activities. This study established a comprehensive framework for the planning of efficient UAV deployments in coastal areas, which was based on recent on-site survey experiences with a portable unmanned aerial vehicle (pUAV) that was carrying a heavyweight spectral sensor. The framework was classified into three main categories: (i) pre-survey considerations (i.e., administrative preparation and UAV airframe details); (ii) execution strategies (i.e., parameters and contingency planning); and (iii) environmental effects (i.e., weather and marine conditions). The implementation and verification of the framework were performed using a UAV–airborne spectral sensing exercise for water quality monitoring in Singapore. The encountered challenges and the mitigation practices that were developed from the actual field experiences were integrated into the framework to advance the ease of UAV deployment for coastal monitoring and improve the acquisition process of high-quality remote sensing images.

Keywords: unmanned aerial vehicles (UAVs); drones; remote sensing; coastal hydro-monitoring; survey planning; comprehensive framework; water quality monitoring



Citation: Trinh, H.L.; Kieu, H.T.; Pak, H.Y.; Pang, D.S.C.; Cokro, A.A.; Law, A.W.-K. A Framework for Survey Planning Using Portable Unmanned Aerial Vehicles (pUAVs) in Coastal Hydro-Environment. *Remote Sens.* **2022**, *14*, 2283. <https://doi.org/10.3390/rs14092283>

Academic Editor: Jorge Delgado García

Received: 11 March 2022

Accepted: 4 May 2022

Published: 9 May 2022

Publisher's Note: MDPI stays neutral with regard to jurisdictional claims in published maps and institutional affiliations.



Copyright: © 2022 by the authors. Licensee MDPI, Basel, Switzerland. This article is an open access article distributed under the terms and conditions of the Creative Commons Attribution (CC BY) license (<https://creativecommons.org/licenses/by/4.0/>).

1. Introduction

Regular coastal monitoring, which includes the monitoring of coastal erosion and air and water quality, as well as the mapping of coastal topography, bathymetry or marine habitats, requires a vigilant and practical observation approach. Over the past few decades, the monitoring of coastal hydro-environment over large spatial areas has been accomplished primarily via either remote sensing with satellite imagery or in situ point-based measurements. While the former method is susceptible to cloud interference [1] and infrequent acquisition times, the latter method is typically costly and time-consuming for continuous acquisition. Remote sensing with unmanned aerial vehicles (UAVs), which are also referred to as uncrewed aircraft systems, holds immense potential in bridging the gap between satellite observations and traditional point measurements, such as fixed-location sampling or in situ grab sampling. With high rates of accuracy and refined spatial resolutions, UAV–airborne sensor systems are efficient tools for the on-demand monitoring of various coastal

applications, such as tracking oil spills, monitoring land reclamation progress, wetland mapping and water quality monitoring [2,3]. However, the deployment of such systems in coastal areas is challenging since marine conditions are constantly changing. In fact, there are many uncertainties in hydro-meteorological variables and in situ survey conditions that can affect the quality and reliability of the acquired data. Diligent operation planning is required to ensure the safety of operations and the quality of the acquired data when conducting UAV surveys in coastal areas. Therefore, a standard and insightful framework for UAV operation is necessary for effective and safe flight surveys over coastal areas.

The existing protocols for UAV flights relate to aerial photography acquisition techniques, survey scales, the resolutions of the final UAV-acquired images and the categorization of parameters, including the parameters of the UAV and the sensor, as well as environmental parameters. Finkbeiner et al. [4] established guidelines for benthic habitat mapping that categorize the processes of image acquisition. These guidelines include mission specifications, environmental considerations, ground control point selection and image analysis. Vize and Coggan [5] compared the pros and cons of different methods that are used in remote sensing techniques to achieve high-resolution data collection, such as satellite and airborne hyperspectral imaging and LIDAR systems. They also presented protocols for seabed habitat mapping. A recent study by Dufy et al. [6] considered the impact of weather and local challenges on flight planning decisions for different locations (i.e., tropical forests, coastal areas, deserts and remote arctic regions) and shared their general suggestions that were based on the site-specific experiences. Ratcliffe et al. [7] provided a brief protocol for the acquisition of aerial images of habitat distribution (e.g., penguin colonies) using UAVs and analyzed the advantages of UAV surveys and limitations due to weather constraints. Another protocol for UAV operation was presented by Doukari et al. [8], in which the authors categorized the protocol into several variables, such as: the location of the study area, in situ data acquisition, environmental conditions and flight parameters. They created a flight toolbox for the Windows operating system that is named the UASea Toolbox, which can assist the operator in UAV planning.

Previous studies have shown that a well-planned protocol is crucial for the successful deployment of UAV systems, particularly in remote sensing applications. However, in recent studies on UAV operation for water quality monitoring (e.g., [9–13]), an explicit and standardized procedure for deploying UAV–airborne spectral systems in coastal hydro-environment has not been mentioned. Additionally, most of the aforementioned protocols were developed for the operation of small and moderately sized UAVs. For the quantitative monitoring of coastal environment, larger UAV–airborne sensor systems, such as hyperspectral sensors, are necessary for certain applications and the operation of these systems is more restricted in terms of time and space due to their heavier payload, which requires meticulous planning and additional safety procedures, such as emergency management and salvage planning. However, these factors were not considered in the previously mentioned protocols. Therefore, this study established a comprehensive framework for the planning of UAV deployment for coastal monitoring, which was based on recent on-site survey experiences with hyperspectral imaging.

To illustrate the benefits of the framework, this paper presents several examples of the monitoring of coastal turbidity during marine operations as part of the Environmental Monitoring and Management Planning (EMMP) in Singapore. In particular, considerations for the administrative proceedings and airframe configurations (e.g., payload vs. maximal endurance) were included in the pre-survey preparations prior to the operation. Moreover, the execution strategy detailed the operational parameters (i.e., flight, UAV and sensor parameters) and contingency planning in accordance with the marine and weather conditions. Finally, the safety thresholds of *p*UAV operation were generated based on an analysis of those parameters and considerations, which assured that high-quality images could be acquired in a safe and efficient manner. The framework of UAV survey planning that was established in this study could serve as the primary guidelines for the seamless deployment of UAVs for coastal water quality monitoring. This study aimed to develop

robust procedures for the deployment of UAVs for coastal water quality monitoring, as well as the acquisition of high-quality images and data from those UAV surveys. As far as we are aware, this study was the first work to establish a comprehensive framework that addresses the challenges for the UAV monitoring of coastal hydro-environment and provides contingency planning for the deployment of heavier and more complicated hyperspectral UAV systems. The research and development of the framework was carried out using our on-site field surveys from over the last two years and the results validated the usefulness of the framework for future related studies.

2. Materials and Methods

2.1. Case Study and Equipment

This framework for UAV-based surveys was developed based on our field experiences from EMMP exercises that monitored land reclamation in a coastal region of Singapore. The study area is located at the southwestern tip of Singapore (Figure 1). During the survey period, intensive coastal operations, including dredging and reclaiming, were carried out in the study area, which induced sediment plumes with high turbidity in the water. UAV flights were conducted to acquire images of the sediment plumes while in situ measurements were acquired from a boat via two methods: grab sampling and a water quality probe. All the UAV flights were conducted in the inner basin of the Singapore Strait, where the water depth is less than 20 m; thus, the marine conditions were calmer than in the open channel of the Singapore Strait.

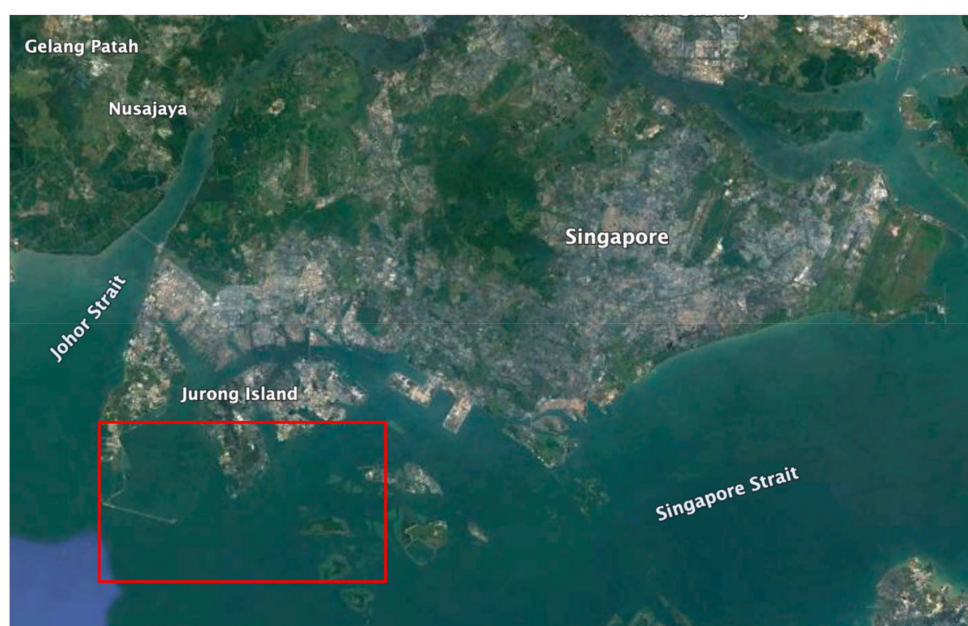


Figure 1. Survey area is located in the inner basin of the Singapore Strait and is indicated by the red box.

All of the UAV flights, in situ measurements and water sampling were carried out during the daytime, between 10:00 and 17:00. The in-situ measurements, such as wind speed and temperature, and the water sampling, as well as the turbidity probe deployment, were all operated simultaneously and within 10–12 min of each UAV flight. The objective of the exercise was to monitor the spatial distribution of turbidity plumes that were induced by dumping or dredging activities in order to avoid transboundary pollution and the output of the exercise was to generate a georeferenced map that showed the distribution of turbidity over the targeted survey area for on-demand monitoring. Turbidity was chosen as a surrogate water quality parameter for the concentration of total suspended solids (TSS). To record the turbidity measurements, a YSI ProDSS Multiparameter Digital Water Quality

meter with GPS capability (Xylem Inc., New York, USA) was mounted to the side of the sampling boat to continuously log turbidity measurements as the boat moved around in the flight area.

To conduct the UAV surveys, a rotary-wing DJI Matrice M600 Pro [14] was chosen as the airborne system to fly over the survey area. The UAV carried a BaySpec OCI™-F push-broom hyperspectral camera [15], as shown in Figure 2, to perform the hyperspectral imaging of the coastal waters, which could provide a broad range of spectral data within the visible to near-infrared (VIS-NIR) spectrum. A total of four surveys, which consisted of eight UAV flights, were conducted from August 2021 to January 2022 in the survey area. After each survey, the hyperspectral images were analyzed, and the framework was further refined to improve the image quality in subsequent surveys.



Figure 2. The UAV–airborne imager system (a) that was applied in the study consisted of the DJI Matrice M600 Pro with Ronin MX gimbal (b), a D-RTK GNSS system (c) and a BaySpec OCI-F hyperspectral camera (d) with visible and near-infrared (VNIR) spectrum capabilities.

2.2. UAV-Based Remote Sensing Framework

A theoretical framework for UAV surveys for monitoring coastal hydro-environment is presented in Figure 3, which summarizes the classification of all factors that affect the quality of the acquired aerial data and the safety of operations. The administrative preparations include obtaining the essential licenses and permits that are required for UAV operation to ensure compliance with all local regulations prior to the UAV surveys. The execution strategy includes UAV and sensor parameterization, survey planning and, especially, contingency planning for emergency events. The environmental conditions are classified into two categories: weather conditions (e.g., windspeed, cloud cover and relative humidity) and marine conditions (e.g., sun glint, marine vehicles and wave and tidal conditions). These categories within the UAV survey framework are discussed in detail in the following sections.

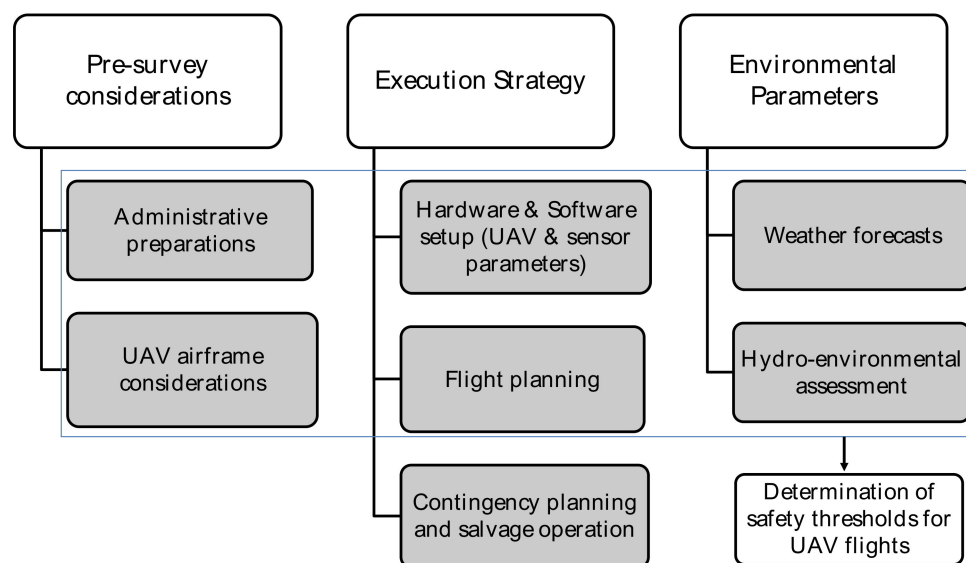


Figure 3. Structure of UAV survey framework for coastal environment.

3. Pre-Survey Considerations

3.1. Administrative Preparation

The administrative preparation involves the legal aspects and local regulations for UAV operation. This includes obtaining the UAV pilot licenses and permits that are required to operate the UAVs legally and safely. In Singapore, the relevant government agencies are the Civil Aviation Authority of Singapore (CAAS) and the Republic of Singapore Air Force (RSAF). Over recent years, civil aviation regulatory bodies worldwide have encountered challenges in managing and updating these regulations due to the extensive use of UAVs and the rapid development of UAV technology [16]. Therefore, national regulations for UAVs need to be promptly developed and adaptively implemented.

3.1.1. Permits and Licenses

The application for permits and other necessary documents for new survey areas is a crucial step in UAV survey planning. The requirements for certain permits and licenses for UAV operation depend on the purposes of the UAVs, i.e., activities under commercial, recreation or education categories. In Singapore, the requirement for operator permits (OP) and activity permits (AP) also depends on the weight category of the UAVs (e.g., >25 kg take-off weight). Furthermore, the UAV operator must hold an unmanned aircraft pilot license (UAPL), which is subject to the specific weight category and purpose of the UAV operation. For instance, a UAPL is only compulsory for UAVs with a total take-off mass above 1.5kg for recreation or education purposes; however, UAV deployment for business activities must be controlled by UAPL holders regardless of the weight of the UAV system.

3.1.2. UAV Regulations

Understanding the regulations for UAV operation is an essential requirement for protecting privacy and public safety. All UAV operation within Singapore airspace is regulated by the CAAS and must comply with the Air Navigation Act (ANA). Specifically, UAV operation must strictly comply with altitude restrictions and acquire the requisite permits for operating UAVs within “no-fly” zones. In general, the UAV should follow the basic regulations to ensure safe and legal operation, as stated below:

- UAPL holders should consult the OneMap app (www.Onemap.sg, accessed on 10 March 2022) in permissible areas to operate a UAV. Areas such as controlled airspace or within 5 km of a registered aerodrome disallow drone operation without prior approval;
- UAVs must always fly within visual line-of-sight of the operator (400 m);

- UAVs must be clear of any members of the public who are not associated with the flight operation;
- UAVs should fly below 200 ft above mean sea level (AMSL), which is equivalent to 60 m;
- All UAVs with a total weight exceeding 250 g must be registered with CAAS before operation.

3.2. UAV Airframe Considerations

3.2.1. Airframe Configuration

A UAV system is fundamentally composed of an aircraft frame, batteries, an onboard autopilot, a propulsion system and a ground control station. A UAV can be remotely piloted using a radio control device at one or more ground control stations that can receive flight outputs, such as the position, altitude, velocity and battery life of the aircraft, via a telemetry radio link. Alternatively, systems can be operated autonomously using an onboard autopilot that can follow a pre-planned flight pattern by processing coordinate and altitude information that is retrieved from satellites or global navigation system (GNSS) receivers and inertial measurement units (IMU). In autonomous flight mode, the UAV operator monitors the UAV motions during the autonomous UAV flights and can interfere manually in emergency situations.

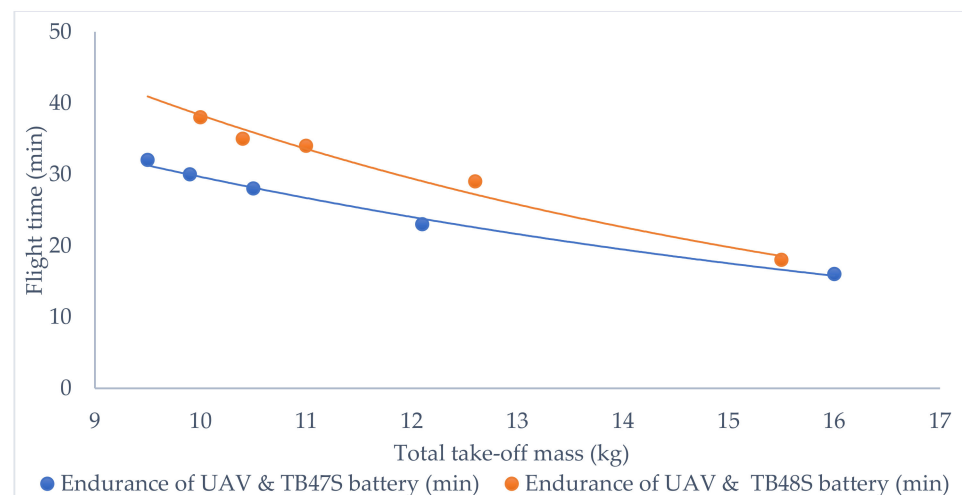
UAV platforms that are commonly used in remote sensing for coastal environment can be classified into two main categories [2]: (1) a multi-rotor system, which is called a portable UAV (*pUAV*) (e.g., octocopters, hexacopters, quadcopters, etc.); and (2) a fixed-wing airframe system (*fUAV*). The key features of these platforms are shown in Table 1. Each airframe system has specific advantages, depending on the purpose for the UAV usage and the environmental surroundings in the survey area. An *fUAV* airframe with a linear flight path is commonly used for routine topographic surveys along coastlines with long (longshore) and narrow (cross-shore) geometries [16]. Moreover, these systems can be easily transported and mobilized since the wings can be separated from the body of the aircraft. By contrast, the *pUAV* platforms are more maneuverable than fixed-wing platforms and are commonly used for monitoring the square patterns of coastal regions. Additionally, as *pUAVs* can mobilize at much lower speeds or even hover at one location, they can allow close and on-point investigation, which is usually required for advanced sensors (e.g., hyperspectral cameras) to obtain better quality images. Furthermore, *pUAVs* can also improve the stability of the camera position through the use of supporting frames, such as gimbals. Thus, the *pUAV* system was chosen in this study. Specifically, a DJI Matrice M600 Pro was chosen as the airborne system to carry a BaySpec OCI™-F push-broom hyperspectral camera. Specifications of the *pUAV*–airborne hyperspectral sensor system can be seen in Table A1.

3.2.2. Payload and Maximal Endurance

The UAV airframe systems can carry external payloads, such as sensors, gimbals, and positioning equipment, for different purposes and missions. The loading capacity of a UAV system is the maximum payload that can be carried by the UAV airframe. The total weight of the basic UAV airframe and the external payload must not exceed the maximum take-off mass. In fact, the payload can affect the capabilities of the UAV in terms of flight endurance, maneuverability, and wind resistivity. Figure 4 indicates the correlation between extended flight times and the variability of take-off mass for the DJI Matrice 600 Pro, for which an increased total take-off mass correlated to decreased flight endurance. The flight times could decrease from 32–38 min for the DJI M600 Pro without payload to 16–18 min for the same UAV system with maximum payload. Appendix A states the specifications of the *pUAV*–airborne hyperspectral sensor system.

Table 1. Configurations of the two popular types of UAV platforms for coastal applications.

	Multi-Rotor Platform (pUAV)		Fixed-Wing Platform (fUAV)	
	Vélez-Nicolás et al. [17]	Device used in this study (i.e., DJI M600 Pro)	Vélez-Nicolás et al. [17]	Device for reference (i.e., Sensefly eBee)
Wingspan	35 to 150 cm	167 cm	157cm	96 to 116 cm
Maximum Take-off Mass		15.5 kg (Including payload)		1.7 kg (Including payload)
Maximum Endurance	15 to 50 min	18 min	15 to 50 min	40 to 45 min
Crush Speed (No wind)		Max 18 m/s		12 to 25 m/s
Wind Resistivity	10 to 15 m/s	8 m/s	8 to 20 m/s	12.8 m/s
Spatial Coverage	20 to 40 ha	4 ha (Flight altitude: 60 m)	80 to 320 ha	30 ha (Flight altitude: 60 m)
Maneuverability		High		Medium
Take-off/Landing Capability		Able to take-off or land vertically (VTOL)		Require a runway (e.g., 100 m) or catapult or hand launch

**Figure 4.** Correlation between the total take-off weight and maximum endurance of a DJI M600 Pro (source: www.dji.com, accessed on 16 February 2022).

There are several other factors that can affect the maximum endurance of a UAV system, such as the specifications of the power supply. For example, TB47S batteries are lighter in weight (595 g) than TB48S batteries (650 g) but the flight times are shorter, as shown in Figure 4. The capacity (4500 mAh) and energy (99.9 Wh) of TB47S batteries are also lower than TB48S batteries, which have 5700 mAh of capacity and 129.96 Wh of energy. Therefore, it is essential to consider the trade-off between the total payload and flight times to achieve specific mission goals.

4. Execution Strategy

The execution planning for a UAV flight is the most important step, which dictates the success of the operation and the quality of the images. Typically, flight parameters, such as height, velocity and the sensitivity of the UAV sensor to obstacles and flight patterns, can be pre-defined using commercial software. Nevertheless, the determination of the parameters requires meticulous calculations that are subject to the mission of the flight and the capability of the UAV system [18]. In the following sections, we address all of these

features and provide guidelines that can be referenced by other operators when conducting UAV surveys with similar airframe setups in coastal environment.

4.1. Parameters for Flight Planning

The parameters that should be considered in a UAV flight plan are classified into two main categories: the UAV and sensor parameters and the flight parameters.

4.1.1. UAV and Sensor Parameters

The basic structure of a UAV system comprises the main airframe body, motors, propellers, batteries, electronic speed controllers (ESC) and a flight controller (IMU). These components must be examined carefully before every flight. The airframe system also includes a payload, as detailed in Section 3.2, and a ground control station that should be equipped with software for flight visualization. The software controls the flight path of the aircraft, as well as the implementation of the entire flight operation. Table 2 shows the settings of the UAV–airborne sensor system that was used in this study.

Table 2. Flight and sensor parameters for the UAV system that was used in this study.

UAV Airborne System: DJI M600 Pro and BaySpec OCI™-F Hyperspectral Imager	
Flight Mode	Waypoints (Scan mode perpendicular to course)
Flight Duration	~11 min
Velocity	5 m/s
Flight Height	60 m AMSL
Image Overlap	~30
Flight Lines	~1 line/10 m of the dimension
Flight Angle	107 degrees

In any UAV survey for imaging, the sensor parameters, including focus, exposure time and sensor gain level, must be calibrated accurately. Specifically, it is critical to calibrate the camera exposure time prior to image acquisition, based on the prevailing light intensity on the day of the survey. Other camera parameters, such as focal length, shutter speed and aperture, are crucial for the improvement of the quality of the aerial images [8]. From these camera parameters, the operator can determine and adjust the ground resolution (cm/pixel), percentage of adjacent image overlap and camera pitch angle during the planning of the flight. Our surveys with the BaySpec VNIR Push-Broom OCI-F hyperspectral camera showed that an overlap ratio between adjacent images of at least ~60% was needed to achieve good image quality. In addition, the analysis of the captured images of turbidity in coastal areas could be affected by multiple factors in the coastal environment, especially the light condition during UAV operation. Therefore, the sensors had to be calibrated prior to the image acquisition process. For the BaySpec hyperspectral camera, a 95% reflectance white reference was used to calibrate the hyperspectral sensor for radiometric correction during the pre-processing of the images. To ensure high-quality image acquisition in the coastal hydro-environment, the calibration process for the sensor (BaySpec OCI-F hyperspectral sensor) had to adhere to the following standard protocol, which was generated from the actual field experiences:

1. Place white reference paper under the camera and ensure that it covers the entire field of view of the camera;
2. No shadow should be cast on the white reference paper. When necessary, the angle of the drone should be adjusted to ensure that the camera and the white reference paper are pointing toward the source of light;
3. During the calibration, auto-exposure should be performed when illumination is the brightest. However, the exposure time should be fine-tuned by adjusting camera gain according to the light conditions;

4. When the exposure time is more than 10 m/s, camera gain should be increased to lower the exposure time. However, when camera gain is already at the maximum, exposure time should be manually set at ~ 10 m/s to minimize interference;
5. Calibrate with dark reference (e.g., using the camera cover) after calibrating with the white reference, while maintaining the gain and exposure time;
6. The Global Positioning System (GPS) of the sensors must be connected and its flight altitude set to the same height as the height of the UAV in the flight planning app;
7. Ensure that the focus of the camera is set to infinity.

4.1.2. Flight Parameters

All of the flight route parameters, such as flight height, velocity and sensor exposure, are pre-defined in the UAV flight planning software (e.g., DJI GO). However, the determination of each parameter requires rigorous calculations, which depend on the capability of the UAV system and the objectives of the UAV flights. In UAV flight planning, the first step is to decide whether the flight should be autonomously or manually controlled. Autonomous missions are popular for mapping and data acquisition (e.g., aerial mapping for water quality monitoring) and are supported by a variety of open-source and commercial flight planning software. This flight mode can achieve consistent frontal and side overlaps for the accurate stitching of high-resolution images. The flight mission is composed of waypoints and a pattern of lines on a reference map, which the UAV system follows to acquire the necessary data. It also includes other parameters of the flight, such as flight height, UAV speed control and camera trigger.

The flight path of the DJI M600 Pro operation during one of the field surveys is shown in Figure 5. The UAV was programmed to follow the path, as indicated by the blue arrow to the starting position. Then, a sequence for the horizontal scanning of the flight area was carried out, after which the UAV was programmed to return to the home point via the path that is indicated by the red arrow. In addition, flight missions have to include considerations of the flight altitude, pixel resolution, number of images, image overlap and side overlap. In this study, the height of the flight above ground level was set at 58 m. The hyperspectral image dimensions were 1280×1024 pixels, and the frontal and side overlaps were 90% and 33%, respectively.

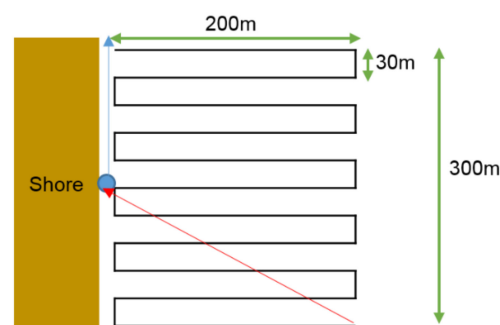


Figure 5. Example of a *p*UAV flight pattern: the take-off/landing point is indicated by the blue dot; the flight path to the starting point is indicated by the blue arrow; the path of the UAV returning to the take-off/landing point is indicated by the red arrow.

4.2. Contingency Planning and Salvage Preparation

Despite well-prepared plans and standardized pre-flight checks of equipment, accidents during UAV operation are still possible due to unpredictable weather conditions or sudden system faults. A discussion on contingency planning was not considered in the previous protocols that address small UAV–airborne sensor systems. However, this planning is compulsory for the larger UAV systems that are typically used for accurate coastal water quality monitoring and arrangements must be in place prior to the start of a flight mission. The contingency measures can be classified into two categories: engineering

controls and administrative controls. The failure of a UAV system could be caused by transmission loss between the remote controller and the UAV (i.e., “lost link”) or engine failure; hence, contingency planning must be in place prior to the start of the UAV flight [19]. Some UAV systems have a built-in function that is activated when transmission is lost during the flight and overrides pilot operation. For example, a DJI UAV can automatically return to the home point when the lost link occurs for more than 10 s. However, even during a UAV mishap, the system must follow a standard operating procedure (SOP) to mitigate the negative consequences (Table 3).

Table 3. Causes and mitigation measures of UAV mishaps.

	Causes	Challenges	Measures
Loss of Communication	<ul style="list-style-type: none"> • Bad weather, such as space weather and heavy storms • Loss of UAV power (e.g., transmitter/remote controller) • Radar jamming or signal interference (e.g., radio, Wi-Fi routers, cellular network, etc.) • Damaged antenna 	<ul style="list-style-type: none"> • UAV capabilities in object detection and avoidance reduction • UAV drifts in the opposite direction and flies erratically 	<ul style="list-style-type: none"> • Constantly tracking stipulated limits of wind speed and weather conditions • Bring UAV closer to the ground station to allow the re-establishing of link • Hover UAV around waypoints away from the planned flight path to let air traffic controller know it is in trouble • Pilot team move to the nearest landing area as soon as possible • Follow pre-planned waypoints and carefully maneuver the UAV to either the nearest landing site or an unpopulated site for landing
Failure of UAV Engines	<ul style="list-style-type: none"> • Batteries run out, causing power loss • Damaged/defected propeller due to harsh weather conditions (thunder, strong wind, etc.) • Overheated motors/ESCs 	<ul style="list-style-type: none"> • Hanging time is short, thus requiring immediate action to maneuver the UAV to landing location 	

In coastal monitoring applications, UAVs need to be configured to adapt to unforeseen failures. Some UAV systems (e.g., eBeeX) are manufactured with a self-inflatable device that allows the system to float on the surface of water in the case of malfunction. Other lightweight UAVs can also be equipped with gliding capabilities or a parachute to avoid crashing/sinking and impacting the marine environment. However, when UAV systems are not equipped with such functions, particularly heavy multi-rotor systems, additional measures should be considered to mitigate environmental impacts in the case of a malfunction that causes the UAV to crash into the sea. There are several mitigation measures that can reduce the retrieval time of a fallen UAV, including the installation of self-inflatable devices (e.g., buoys or floats) [10,20,21] or the use of a tethered ground station to trace and pull the fallen UAV from the seabed via a sturdy cable [22,23]. The selection and deployment of these measures depend on the practical conditions of the survey. Understanding the loading capacity and limitations of the UAV is important for the design of appropriate salvation measures. Moreover, any decisions regarding the rescue and retrieval execution should consider marine traffic during the salvage period to ensure the safety of the operation team. The advantages and disadvantages of each measure are presented in Table 4.

Table 4. Comparison of measures for UAV recovery from water.

Measures	Pros	Cons
Tethered Drone Station	<ul style="list-style-type: none"> • Easy to track and pull the fallen UAV from the seabed via the cable attached to the UAV • Device can supply more power to the drone system as the cable is connected to an on-land power station 	<ul style="list-style-type: none"> • Attachment significantly increases the payload • Limited flight distance based on the cable length • The long cable affects marine traffic • High cost (above USD 25,000) • The attachment depends on the design of the UAV and some UAV systems are not able to be fitted with this device • A boat or vessel is still required to remove the UAV from the water
Water Rescue Device (i.e., float, buoy, etc.)	<ul style="list-style-type: none"> • Affordable (e.g., DR9 water recovery device) • Attachments add 550g to the overall payload of a UAV but they are lighter than a tether 	<ul style="list-style-type: none"> • The floating drone can still impede marine traffic • The waiting time while the rescue team is mobilized causes delays in the rescue activities
Diver and Safety Boat	<ul style="list-style-type: none"> • Manual retrieval operations are more thorough and safer • Reduces waiting time as the team is on standby for immediate rescue action 	<ul style="list-style-type: none"> • Option of standby safety boat and divers is not cost-efficient in the long run because engaging crew and equipment for a salvage operation is charged on a daily basis

In this study, the total take-off mass of the *p*UAV–airborne sensor system DJI M600 Pro reached the limit of 15.5 kg; hence, the engineering measures were not considered. As an alternative, the survey team deployed a standby boat with diving equipment and personnel for salvage operations during every UAV flight. The water quality measurements were also recorded via a turbidity probe that was attached to the side of this boat and grab samples were taken simultaneously.

5. Environmental Factors

A pre-flight assessment of the survey area and the weather phenomena that are prevailing in that area is important for accurate flight planning and the acquisition of reliable data [24]. Weather and oceanographic parameters interact and correlate together and thus, should be considered during marine applications. During UAV surveys, the environmental conditions affect the stability of the UAV and may introduce interferences into the spectral responses during the image acquisition process [6]. Moreover, environmental factors can also affect the accuracy of image processing and the analysis of water quality [11]. Thus, they must be closely monitored during any UAV operation.

The meteorological and environmental factors include atmospheric forecasts (e.g., wind speed, rain, haze, relative humidity, cloud cover, etc.) and hydro-environmental assessments (e.g., sun glint effect, tidal conditions, waves and currents). Specifically, rain conditions and wind speed should be monitored for the in-situ planning and operation of a UAV flight. Sun angle, light intensity and tidal conditions should be monitored as environmental parameters to be fed into the data analysis to examine their effects on the spectral responses of coastal waters. In this study, apart from the in-situ measurements of wind speed, ambient temperature and water temperature, the main source of environmental data that were utilized for the survey was retrieved from the website of the Singapore Meteorological Services (SMS) (www.weather.gov.sg, accessed on 10 March 2022). In this study, apart from the in situ measurements of wind speed, ambient temperature and water temperature, the main source of environmental data that were utilized for the survey was

retrieved from the website of the Singapore Meteorological Services (SMS) (www.weather.gov.sg, accessed on 10 March 2022). This website provides collated environmental data (in 1-min intervals), such as ambient temperature, wind speed and relative humidity, from several weather stations across the island.

5.1. Weather Forecasts

5.1.1. Wind Speed Fluctuations

Strong wind conditions can affect the trajectory and endurance of a UAV. When flying under strong wind conditions, it is harder for a UAV to maintain its flight path. To compensate for disturbances that are created by strong winds, the motors need to produce more thrust to maintain a constant speed and direction. This results in a larger current draw from the batteries, which diminishes the flight time. Furthermore, strong winds can cause disturbances on the surface of water, which can create more interference in image acquisition and affect the image quality. Hence, during our on-site surveys, the pre-flight planning was conducted in the field to assess the impact of wind speed on data quality. In particular, instantaneous and localized wind speeds in the coastal area fluctuate in terms of both speed and direction; thus, in this study, wind speed was measured in 1-min intervals using an anemometer (i.e., RS PRO DT-3893). It was found that reducing the aerodynamic drag of the wind by changing to a fixed mount and/or altering camera mounts and orientations could help to reduce the impact of wind on the drone motions. In addition, using supporting gimbals (e.g., Ronin MX Red [25]) to secure the camera position and mitigate vibrations during image capturing can be extremely effective against wind fluctuations. However, wind speed varies spatially and altitudinally; thus, UAV operators need to monitor the movement of the drone closely to ensure a safe flight and take immediate action if weather conditions change adversely.

5.1.2. Cloud Conditions

Most portable UAVs operate at low altitudes under the cloud level, which allows them to acquire images without being covered by clouds. However, cloud shadows or haze can still result in poor illumination conditions and affect the color contrast of aerial images, which make it difficult to differentiate between benthic features and material discharges (i.e., sediment) from marine operations. Clouds and their shadows can alter the measured spectral responses of water bodies, which may produce unreliable results, particularly in turbidity monitoring. Therefore, operating UAVs under partial cloud cover conditions can lead to changes in illumination conditions when the UAV enters a cloud covered area, as shown in Figure 6, which affects the homogeneity of spectral features (e.g., derived spectral, structural or classification-based data products) [6].

In addition, the stitching process for water surface images can also be sensitive to light intensity variations from cloudy and shady weather due to the adjustments in shutter speed, which thus affects the overlap of the images. Drizzling and low light conditions due to passing cloud cover can cause poor image quality. To address this issue in this study, an additional spectrometer was mounted onboard the UAV system to capture the changes in light intensity during the flight, which were subsequently used for radiometric correction. Nevertheless, spectrometer fluctuations are caused by changes in illumination conditions, such as sudden thunderstorms that reduce the irradiance that is received by the spectrometer. Figure 7 shows the defects in stitched images from poor illumination conditions. These images were acquired during an afternoon flight when a thundercloud occurred in the study area. The dramatic fluctuations in reflectance for spectral bands above 740nm indicate the effects of the poor illumination that was caused by the approaching thunderstorm. The sudden changes in illumination conditions ultimately affected the radiometric correction, as relative radiometric correction is sensitive to initial camera calibration and illumination, which led to poor reflectance results. Hence, once there are signs of heavy cloud coverage or thunderstorms, UAV operators should immediately cease UAV operation.

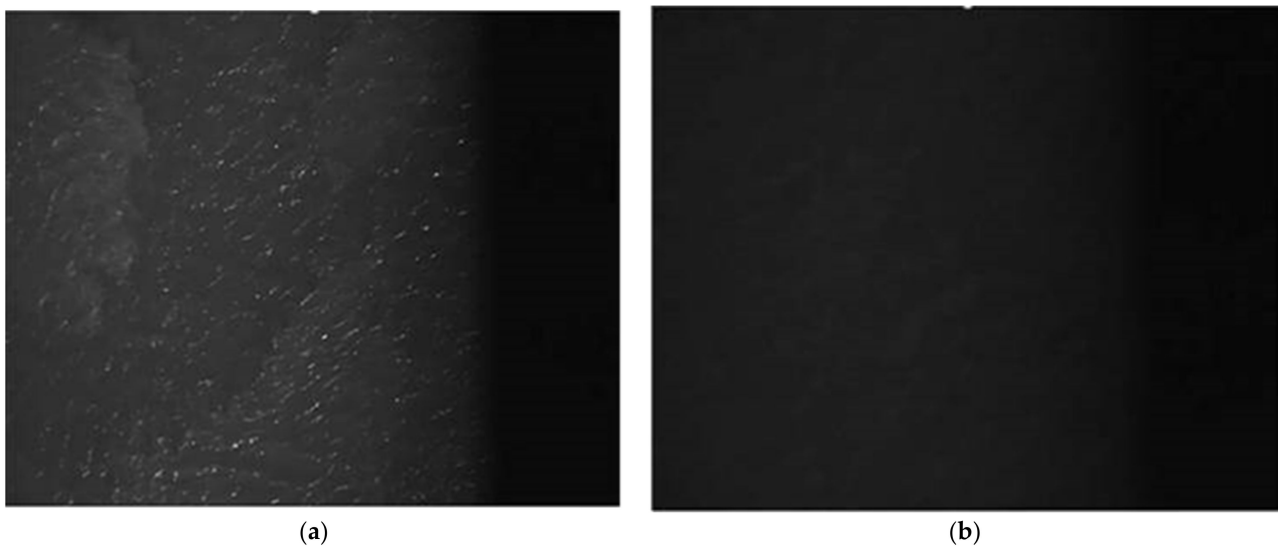


Figure 6. Raw images of survey area during the same UAV flight on 3 May 2021: (a) without and (b) with cloud cover.

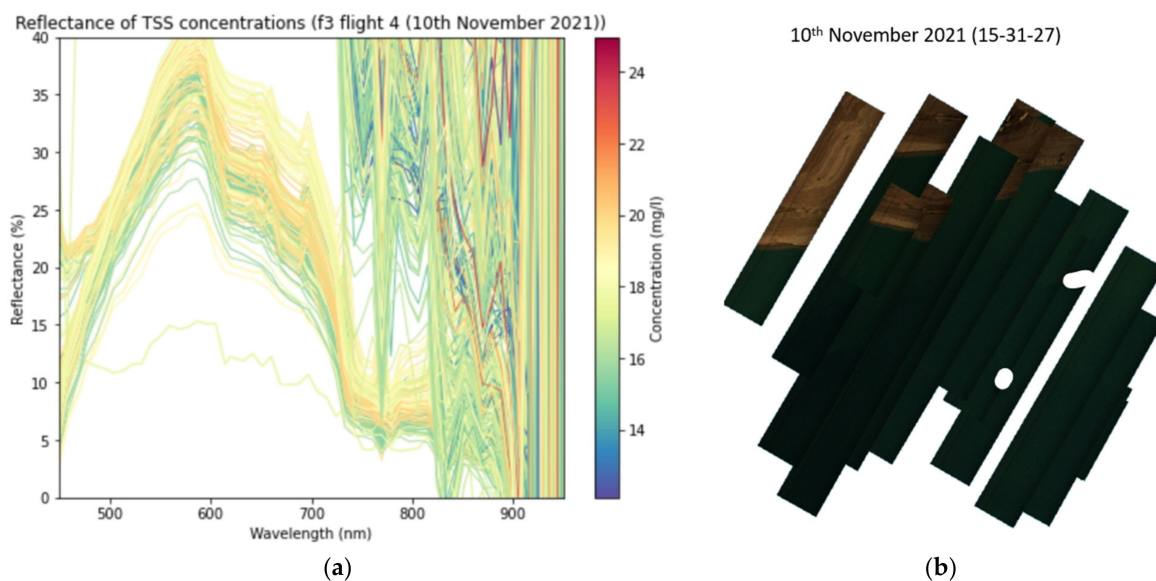


Figure 7. (a) Poor acquired data during a UAV flight at 04:48 p.m. on 10 November 2021 due to shady conditions and a sudden thunderstorm. (b) The stitched images could not be aligned and there are some missing data due to the reduction in camera shutter speed, which was caused by the poor illumination conditions.

5.1.3. Rain and Humidity

In the planning of UAV flights, the occurrence of rain could even suspend the operation. As many commercially available drones are not waterproof, rain and high humidity could damage the UAV. Rain droplets or a high moisture content in the atmosphere can lead to the electrical components in the UAV short-circuiting and the equipment becoming damaged. Due to the possible adverse impacts on UAV operation, the sky conditions during every field survey of this study were visually monitored in conjunction with checking weather forecasts and the nowcast map of rain intensities from several sources, such as mobile apps (i.e., myENV), the Singapore Meteorological Services website (www.weather.gov.sg, accessed on 10 March 2022) and the National Environment Agency (NEA) website (www.

nea.gov.sg/weather/rain-areas, accessed on 10 March 2022). When rain occurred, UAV operation was suspended until the weather conditions improved.

5.2. Hydro-Environmental Assessments

Oceanographic variables are important for marine aerial applications and thus, must be considered during flight planning. Long-term planning allows for comprehensive research and the collection of the necessary oceanographic information, such as turbidity levels, water temperature patterns, tides and the phenology of an area of interest [8]. The oceanographic measurements can either be obtained from local weather stations, where they are available, or via field measurements [24].

5.2.1. Sun Position and Angles

Compared to land monitoring, the UAV imaging of coastal water environment poses more challenges due to the varying solar altitude and azimuth, which can cause specular reflection and result in the appearance of sun glint in the images, thereby affecting the accurate determination of reflectance and discrimination between marine features. In coastal areas, fluctuating wave conditions can also intensify this effect. The solar altitude and azimuth and the sensor angle on the UAV play an important role in the quality of the image since unfavorable solar altitudes and azimuths result in excessive sun glint in the images, which affects the accurate determination of reflectance and prevents discrimination between marine features [6,11]. Information on sun elevation angles can be retrieved from the SunCalc website (www.suncalc.net, accessed on 10 March 2022) prior to each flight to determine the favorable positions. During the actual field surveys with our *p*UAV–airborne spectral system, the sun angle frequently exceeded 75 degrees during the noon period (from 11:30 p.m. to 2 p.m.), which was not ideal for image acquisition over water bodies as the image could be affected by sun glint effect, as shown in Figure 8b. However, a small angle of below 35 degrees, usually in the early morning (before 7 a.m.) or late afternoon, was also unsuitable for image acquisition using the UAV–airborne system. Therefore, operators should conduct flight experiments with varying sun angles (e.g., at different times of the day) and adjust the exposure settings on their UAV–airborne system to optimize the image quality. Time variation is necessary to investigate the presence of sun glint and the effects of light refraction on the apparent position and shape of underwater objects. In our study, radiometric correction was applied to the retrieved spectral reflectance, although the radiometric correction was limited when the hyperspectral sensor experienced oversaturation. To reduce the effects of sun glint, the flight paths were planned to be perpendicular to the solar azimuth.

5.2.2. Tidal and Wave Conditions

Tidal and wave conditions are important marine parameters that have a great impact on the quality and clarity of water and consequently, the quality of aerial data. In Singapore, marine data (i.e., wave height forecasts) can be retrieved from the SMS portal (www.weather.gov.sg, accessed on 10 March 2022), which lists four data points for the duration of 24 h. Another source is the tide atlas on the Maritime and Port Authority of Singapore (MPA) website. In particular, the digital tide atlas provides simulated tidal and current information in 30-min intervals from two anchorages in Singapore (the Sudong Anchorage and the Eastern Bunkering Anchorage). In this study, the survey area is located in the inner basin of the Singapore Strait, where the coastal hydrodynamic conditions are calmer and do not vary significantly. As a result, the dispersion of plumes during the *p*UAV flight operations was slower compared to areas of open channel, where the current is usually higher. Hence, the effects of current speed and wave height were observed but not considered to be significant to the UAV imagery of the sediment plumes in this study. Another marine factor that can affect survey planning is tidal height. Based on local experiences of previous survey areas and sea surface observations, it is recommended to conduct UAV operation for aerial data acquisition during high tide conditions. The tide height should be at least above 0.5 m to

ensure the safety of the marine team when conducting water quality surveys, as well as to ensure the minimum depth of sea to distinguish between the seabed and the images that are captured during UAV operation. In addition, this height also ensures the minimum depth to distinguish between the seabed and other features (i.e., sediment plumes) during dumping or dredging operations.

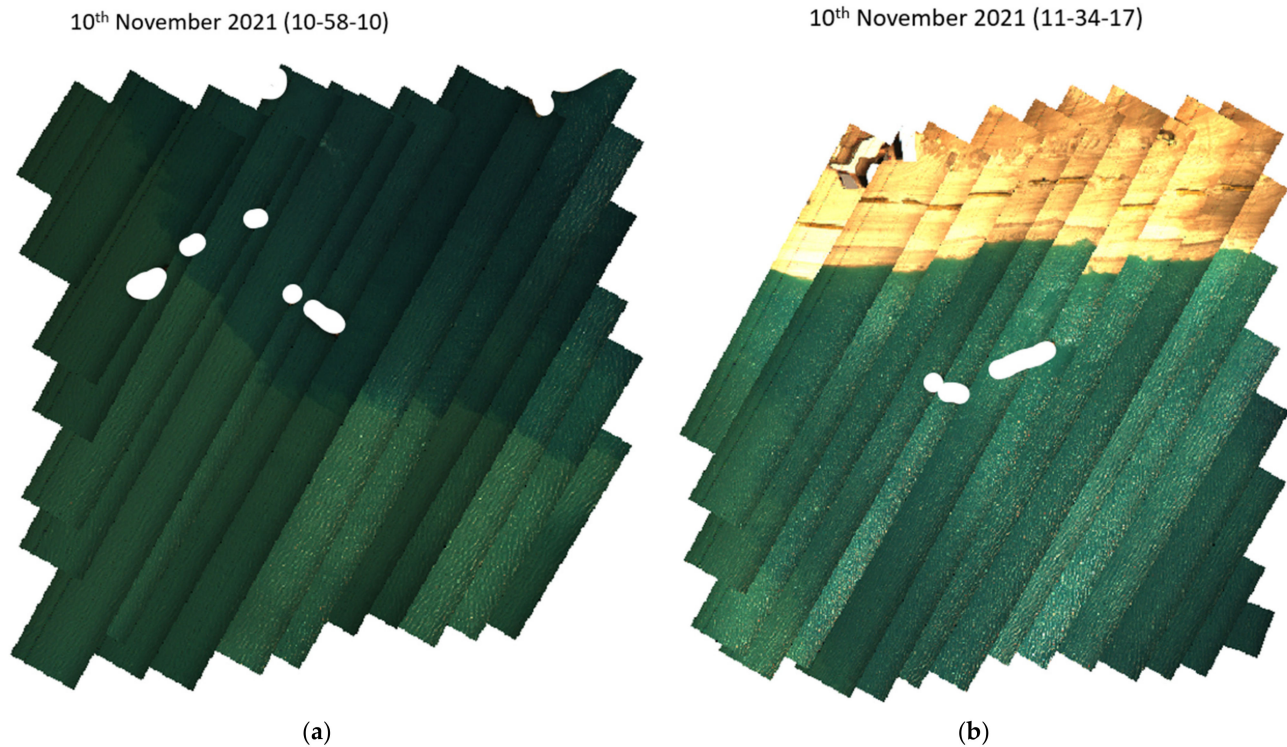


Figure 8. Sun reflectance on water bodies at different times: (a) without sun glint at 10:58:10 a.m. and (b) with sun glint at 11:34:17 a.m. The sediment plume can be seen in the flight area while barge ships/vessels/boats are masked from the stitched image (white areas).

5.2.3. Movement of Marine Vehicles

None of the previous protocols in the existing literature for UAV surveys in coastal environment mentioned the effects of marine vehicles during the data acquisition process. In fact, the appearance of marine vehicles in acquired images is a source of interference in the retrieval of spectral reflectance, as shown in Figure 9a. Hence, when UAVs are operated in congested areas, operators should target water bodies with less traffic to minimize the disruption to their image acquisition. When boats do appear in images, interference removal must be applied during the image processing, as shown in Figure 9b. Moreover, in water quality surveys, sampling boats can be utilized for in situ measurements by collecting water samples or logging water quality data using a probe alongside the deployment of a UAV system. However, these boats can appear in the images that are acquired by the UAV system as well; thus, the area behind the boat may be disturbed by the motor and movement of the boat, which disrupts the in-situ water conditions. To avoid capturing the disturbances that are caused by the movement of the sampling boat, the boat should move in the forward direction and not reverse, as well as following behind the UAV flight path.

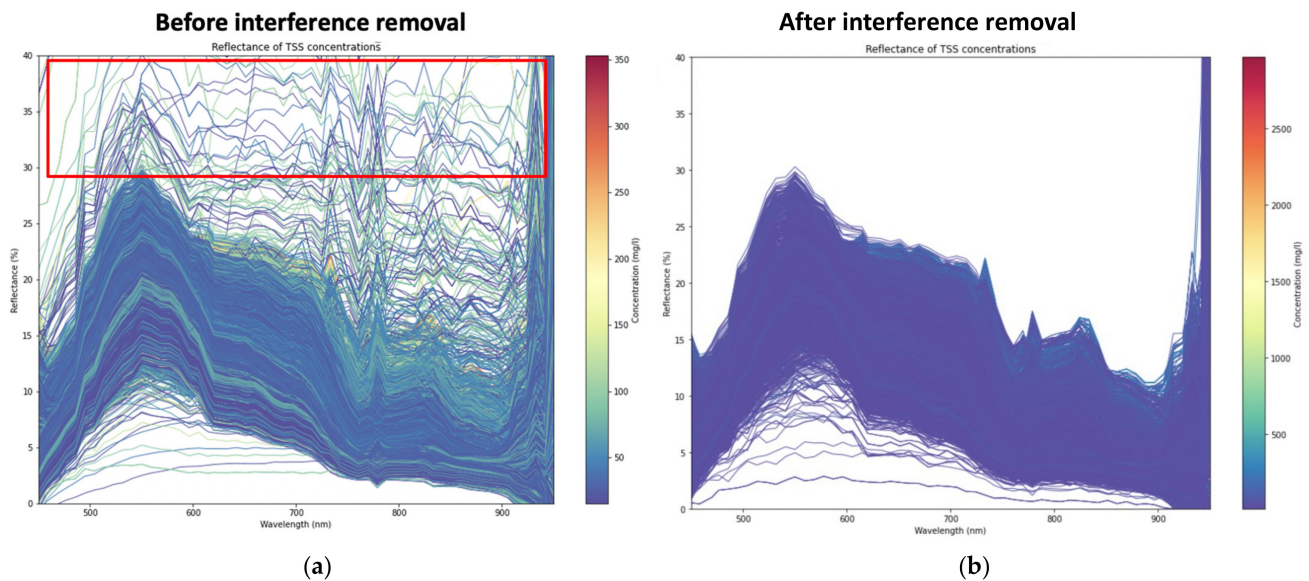


Figure 9. TSS reflectance during UAV flights (a) with noise that was caused by the appearance of barge shown in the red box and (b) with the noise removed.

6. Results and Discussion

6.1. Results

The results in this paper are based on three UAV surveys that were conducted in the study area located in the inner basin of the Singapore Strait during the monsoon season at the end of the year (i.e., November and December), namely on 10 November 2021, 9 December 2021 and 13 January 2022. Table 5 presents a range of hydro-meteorological parameters during three surveys. Due to the fluctuating weather in tropical countries, such as Singapore, there could be persistent strong winds (>8 m/s) and occasional precipitation and high cloud illumination during the monsoon season. From Table 5, it can be observed that the selected UAV surveys were all conducted under dry weather conditions and with wind speeds below 6 m/s, as well as during high tides to avoid the risk of accidents and to ensure that usable data could be obtained.

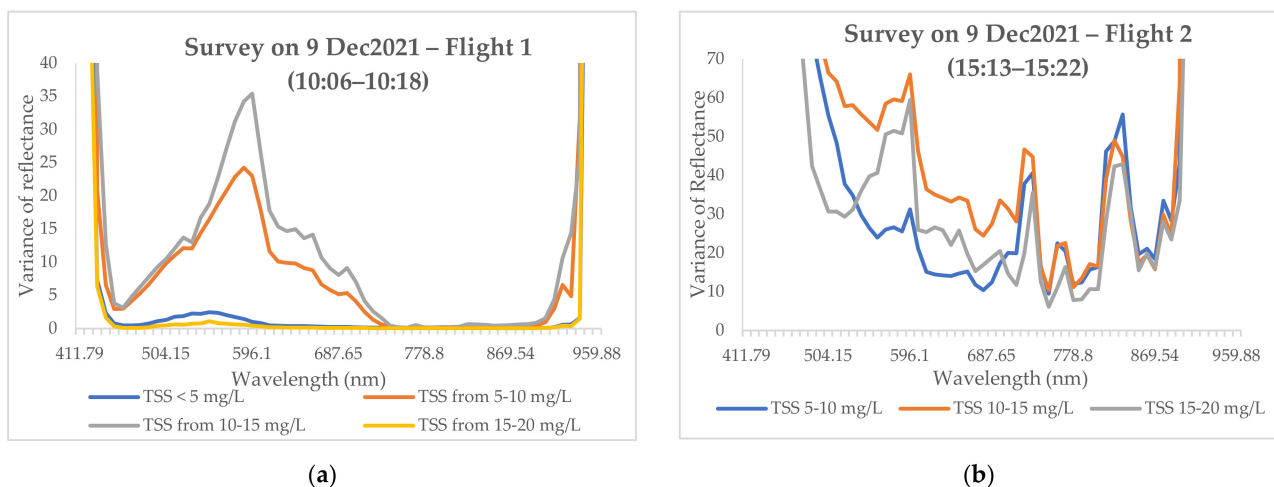
The surveys were all planned in the morning because the possibility of rain and thunderstorms was typically higher in the afternoon, which could lead to poor data acquisition or the cessation of *p*UAV operations. However, weather conditions did not cooperate on 13 January 2022 and afternoon flights had to be conducted. As shown in Table 5, the UAV flight on 9 December 2021 started at the optimal acquisition time of 10:06 a.m. and had a variance of reflectance below 39%, which led to a good imaging outcome, as shown in Figure 9a. By contrast, the flight at 16.13 p.m. experienced dark clouds and developing thunderstorms and rain from the southeast of the survey area. As a result, the images that were acquired were of a low quality, which was demonstrated by the significant fluctuations in reflectance within the 430 to 930 nm range of spectral bands, as shown in Figure 10b.

Figure 10 shows the variance of reflectance during the survey on 10 November 2021. The reflectance spectra in Figure 11b, which were captured under the highest recorded sun angles of all UAV flights (up to 72 degrees), show that the variance of reflectance during this flight was higher than the earlier flight at 10:59 a.m., which had sun angles below 70 degrees. The reflectance varied remarkably within the range of high wavelengths (above 830 nm) as those wavelengths were more sensitive to the oversaturation of the sensor. To mitigate such effects, radiometric correction was performed using a spectrometer to reduce oversaturation during data acquisition under strong light conditions. In addition, the flight path was planned to be perpendicular to the sun angle in order to minimize the sun glint effect [6]. Hence, the results of this flight were considered acceptable for analysis.

Table 5. Summary of weather parameters and reflectance of TSS concentrations that were acquired during UAV field surveys, which we conducted during the period of November 2021 to January 2022.

Flight Time of UAV Survey	10 November 2021		9 December 2021		13 January 2022	
	10:59–11:10	11:36–11:45	10:06–10:18	16:13–16:22	16:04–16:11	16:28–16:36
TSS Concentration (mg/L)	8.3–43.9	5.9–19.89	3.7–11.7	6.3–16.8	4.4–53.9	4.9–122.1
Air Temperature (°C)	27–28	27–28	28–29	26–27	32–33	31–32
Water Temperature (°C)	29.5–30	29.5–30	29–30	29–30	28–29.5	28–29
Relative Humidity (%)	83–85	80–81	71–73	88–94	44–49	43–51
Wind Speed (m/s)	2.3–3.2	3.9–4.2	0.4–4.0	0.9–2.8	1.3–3.9	1.7–3.6
Sun Angle * (degree)	68–70	71–72	53–56	35–37	28–33	35–39
Weather Conditions **	Sunny after rain in the early morning	Strong sunlight with sun glint effect	Sunny	Heavy cloud cover and slight rain	Sunny	Cloudy
Variance of Reflectance (Wavelength in the range of 430–930 nm) ***	0.15–50.1	0.46–32.4	0.015–38.8	6.12–19,947	0.08–4.556	1.14–4.945

* Sun position was retrieved from www.sunearthtools.com, accessed on 10 March 2022, according to the exact coordinates and times of each UAV flight; ** weather conditions were based on the observations and records of the UAV operators during actual field surveys (Figure A1 shows photos of the actual coastal conditions during the UAV flights); *** a range of spectral bands was selected based on the stability of the wavelength during all UAV flights (the reflectance of extreme wavelengths that were lower than 430 nm or greater than 930 nm was not considered in this study).

**Figure 10.** Variance of reflectance for the different groups of TSS concentrations (a) during good weather conditions and (b) poor weather conditions due to cloud contamination and rain.

The concentrations of turbidity were classified into different groups, including low concentrations from 0 to 50 mg/L (Figures 10 and 11) and high concentrations of above 50 mg/L (Figure A2). The variability of reflectance among each spectral band demonstrated the quality of data acquisition, for which high variance corresponded to poor results. The variance of reflectance that was acquired by the UAV–airborne sensor system was independent from the range of TSS concentrations that were captured during the surveys. However, the tendency was for high variance to occur within the range of low to medium TSS concentrations, 5–20 mg/L, for all the UAV surveys.

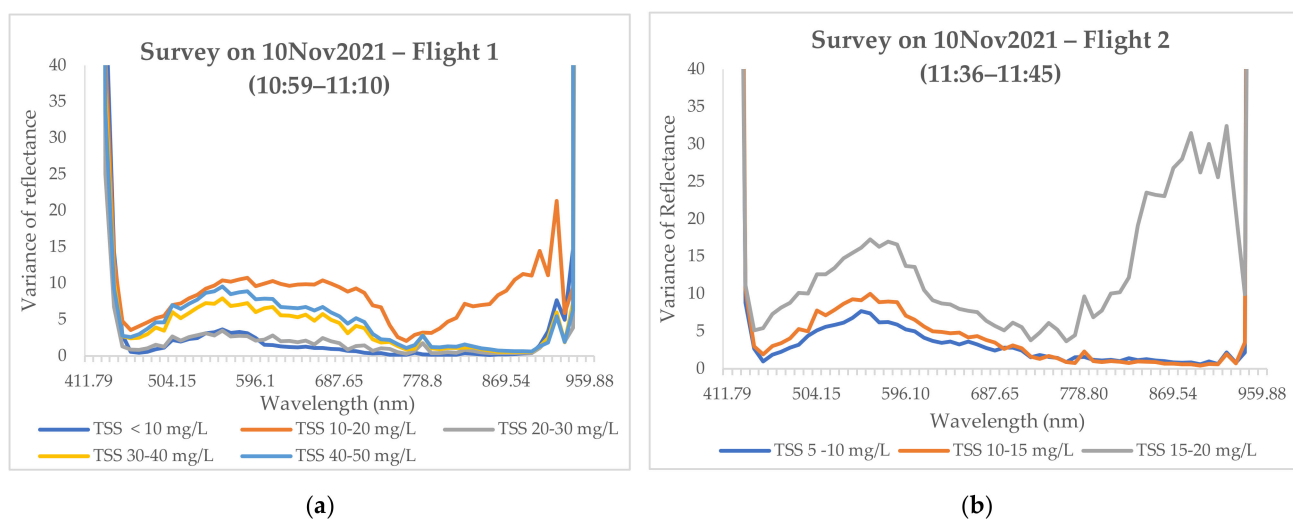


Figure 11. Variance of reflectance of the survey flights during UAV flights (a) without and (b) with high sun glint effect for different groups of TSS concentrations.

6.2. Discussion

The marine and meteorological conditions were observed and measured during 11 UAV flights, which were conducted from May 2021 to January 2022 under both sunny and cloudy weather conditions. However, good results were only achieved from the *p*UAV surveys on 10 November, 9 December 2021, and 13 January 2022, which were performed under ideal weather and marine conditions and strict compliance with the standardized flight setups. The generation of a ruleset for these parameters that is based on the actual field practices would allow us to reproduce the safe and efficient UAV operation with similar UAV–airborne sensor systems in other coastal regions. Hence, the determination of these thresholds is essential for field surveys to reduce the likelihood of malfunctions and crashes that are caused by the loss of telemetry links or low battery power supplies to the UAV systems. The common recovery practice is to program the UAV to return to the home location and land automatically in the case of lost communication with the ground control station or in the case of the battery percentage dropping below a pre-set level. For example, commercial *p*UAVs usually allow a flight time of under 50 min as their maximum flight endurance (as shown in Table 1). Thus, the flight height and speed should be adjusted to ensure that the flight covers the entire survey area within the safe zone. As shown in Figure 4, when the total weight of our UAV–airborne sensor system reached 15.5 kg, the maximum endurance of the UAV flight decreased to less than 16 min. Due to the heavyweight payload on the *p*UAV system that was used in this study, the flight duration was kept to under 12 min to ensure safe operation. Based on the operation experiences with the weather parameters that were recorded in Table 5, we summarize the recommended hydro-meteorological guidelines for aerial marine image acquisition using the UAV–airborne sensor system of a DJI M600 Pro and BaySpec OCI™-F Hyperspectral Imager in Table 6. Specifically, the wind speed threshold must be considered in accordance with the airframe configuration and the total payload. In our case, the wind speed threshold for the deployment of the *p*UAV could not exceed 8 m/s. Other environmental parameters should also be considered on the date of UAV operation. Specifically, the recommended sun angle should be lower than 75 degrees to avoid sun glints but higher than 35 degrees to ensure sufficient light conditions for remote sensing. The sky should be bright and clear with a cloud cover of below 25% [25] or at least avoiding partial cloud cover, which can result in inconsistent image acquisition. Eventually, the default thresholds that were generated for Table 6 will be applied in subsequent surveys using the hyperspectral UAV system to provide accurate spectral imaging of coastal water bodies in order to understand the turbidity distributions in the study area.

Table 6. Safety thresholds of weather variables for the safety and good image quality of *p*UAV operation.

Parameters	Thresholds
Wind Speed (m/s) *	<8
Air Temperature (Celsius)	<35
Water Temperature (Celsius)	<30
Relative Humidity (%)	<85
Sun Angle (degree)	35–75
Tidal Height (m)	>0.5

* Wind speed is considered based on in situ measurements at the points of UAV take-off/landing.

Nevertheless, despite adherence to the aforementioned safety thresholds, the image stitching of UAV images over coastal regions is more challenging compared to land monitoring images due to the low number of features and the homogeneity of the water surface. These factors significantly affect the efficiency of feature-based stitching algorithms and sometimes even result in the failure of the image stitching procedures. When UAV–airborne sensor systems are deployed over inland water bodies, surface features, such as water banks, can be used as distinctive features for feature-based image stitching algorithms [26]. However, coastal environment lack such distinctive features; thus, a feature-based stitching algorithm cannot be employed satisfactorily. Since ground control points (GCPs) cannot be placed on the water surface, georeferencing using a high number of GCPs is also very challenging [27]. We found that the most useful approach for coastal environment was to perform image georeferencing based on the GPS coordinates that were recorded by the GPS module in the camera. The georeferenced images could then be imported as layers in GIS for further processing and mapping applications. At the same time, the retrieval of the GPS data was crucial for this approach. For the analysis in this study, an original stitching algorithm was developed to process and stitch the homogenous hyperspectral raw images of the water surface. Examples of the stitched and georeferenced images can be seen in Figure 8. The georeferencing and georectification development for this stitching software is still in progress, which will be detailed in future studies.

7. Conclusions

Remote sensing using UAV–airborne spectral sensor systems exhibits tremendous potential, as the approach provides high-resolution image acquisition for a wide range of coastal applications, especially water quality monitoring. The comprehensive framework for UAV surveys that was established in this study can enable safe and efficient UAV operation in the coastal hydro-environment, especially for heavyweight and complicated UAV systems such as *p*UAV–airborne hyperspectral sensor systems. Detailed considerations, such as administrative preparations, airframe settings as well as impacts of hydro-meteorological variables on the execution strategy and contingency planning, are included in the proposed framework, which can significantly contribute to successful UAV flights and optimal data acquisition. The framework was validated via the acquisition of high-quality images through safe operation during actual field surveys in Singapore. The analysis in this study defined the effects of in-situ conditions on UAV operations and image quality. Moreover, the challenges for the stitching of images over homogenous water bodies were overcome by employing a GPS-based image stitching method. Future studies will be pursued in varying coastal conditions with the inclusion of more advanced UAVs or spectral sensors to further enhance this framework.

Author Contributions: Conceptualization, H.L.T., H.T.K. and A.W.-K.L.; methodology, H.L.T., H.T.K., H.Y.P. and A.W.-K.L.; formal analysis, H.L.T., H.T.K. and H.Y.P.; data curation, H.L.T., H.T.K., H.Y.P. and A.A.C.; writing—original draft preparation, H.L.T.; writing—review and editing, H.T.K., H.Y.P., D.S.C.P., A.A.C. and A.W.-K.L.; visualization, H.L.T. and H.Y.P.; supervision, A.W.-K.L.; project administration, H.L.T. and D.S.C.P.; funding acquisition, A.W.-K.L. All authors have read and agreed to the published version of the manuscript.

Funding: This research was funded by the Singapore Maritime Institute (SMI) under the research project “UAV-based Remote Sensing of Turbidity in Coastal Waters”, grant number SMI-2020-MA-02.

Institutional Review Board Statement: Not applicable.

Informed Consent Statement: Not applicable.

Data Availability Statement: The weather dataset is available for download at Singapore Meteorological Services website (www.weather.gov.sg, accessed on 10 March 2022) and the National Environment Agency (NEA) website (www.nea.gov.sg/weather/rain-areas, accessed on 10 March 2022). The information of sun elevation angle is available for download at the SunCalc website (www.suncalc.net, accessed on 10 March 2022).

Acknowledgments: The authors would like to acknowledge the contributions of the Maritime and Port Authority of Singapore (MPA) and DHI Water and Environment (S) Pte Ltd., as well as Surbana Jurong Pte Ltd. (SJ).

Conflicts of Interest: The authors declare no conflict of interest.

Appendix A

Table A1. Specifications of the *p*UAV–airborne hyperspectral sensor system.

Component	Model/Number	Specification	Weight (kg)
Portable Rotary-UAV (Battery included)	DJI Matrice M600 Pro [14]	<ul style="list-style-type: none"> • Maximum flight height: 2500 m • Maximum flight time: 18 min • Maximum payload: 5.5 kg • Maximum wind resistance: 8 m/s 	9.5 (With six TB47S batteries)10 (With six TB48S batteries)
Hyperspectral Sensor	BaySpec OCI-F Hyperspectral Camera [15]	<ul style="list-style-type: none"> • Sensor type: Push-broom scanner • Spectral range: 400–1000 nm • Number of spectral bands: 61 • Spectral resolution: 10–12nm • 16 mm lens • Spatial pixel resolution: 1024 × scan length 	0.6
Gimbal Stabilizer	DJI Ronin MX Gimbal [28]	<ul style="list-style-type: none"> • Angular vibration range: $\pm 0.02^\circ$ • Maximum controlled rotation speed: Yaw axis: $200^\circ/s$; Pitch axis: $100^\circ/s$; Roll axis: $30^\circ/s$ • Rotation range: Pitch: -150°–270°; Roll: -110°–110°; Yaw: 360° 	4.5
Georeferencing System	D-RTK GNSS System [29]	<ul style="list-style-type: none"> • Positioning accuracy: Horizontal: 1 cm + 1 ppm; Vertical: 2 cm + 1 ppm • Root mean square (RMS): 0.03 m/s • Input voltage: 3S to 12S (12 to 52 V) 	0.14
Onboard Calibration Spectrometer	Ocean Optics Flame-SVIS-NIR Spectrometer	<ul style="list-style-type: none"> • Wavelength range: 350–1000 nm • Optical resolution: 1.33 nm FWHM • Integration Time: 1 ms–65 s 	0.3
Mini PC for Data Storage	Intel NUC	<ul style="list-style-type: none"> • CPU: Intel Core i5 • Storage capacity: 500 GB 	0.48
Power Supply for Spectral Sensor	Omni Mobile 25600 Charger [30]	<ul style="list-style-type: none"> • Power source: 96 Wh • High-capacity battery: 25,600 mAh • Built-in smart power controller, including solar recharging function 	0.58
TOTAL WEIGHT			15.5–16

Appendix B



Figure A1. Actual photos taken during the survey on 9 December 2021 under (a) good weather conditions and (b) bad weather conditions due to the approaching thunderstorm and rain.

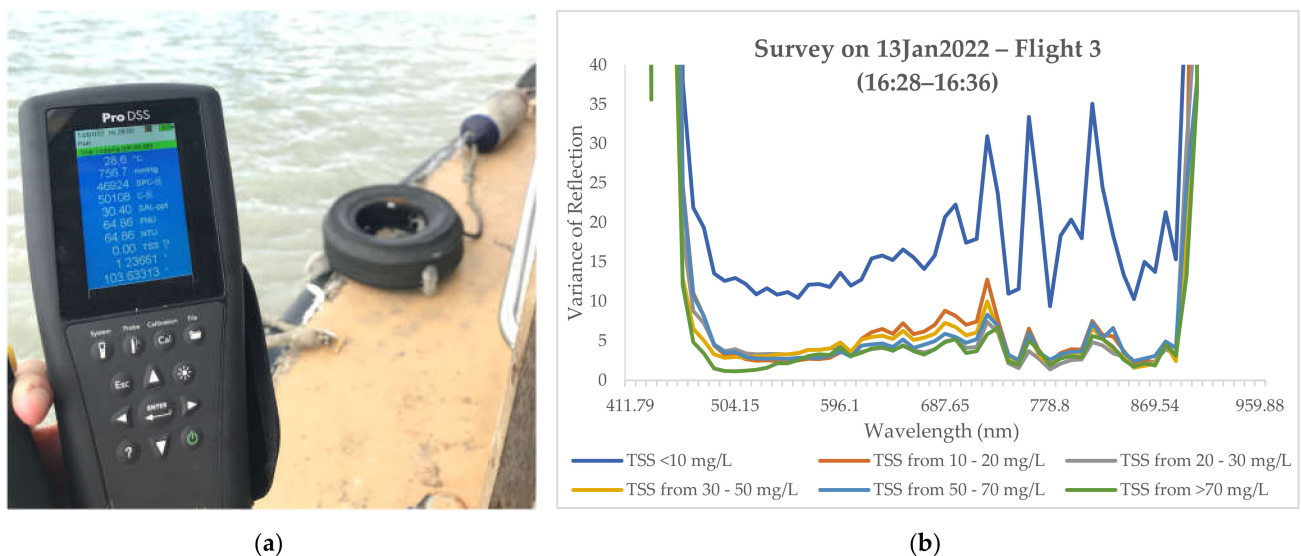


Figure A2. (a) Flight at 4:28 p.m. on 13 January 2022 recorded the highest TSS concentrations of up to 122 mg/L because the sediment plumes were captured near a discharge source, i.e., a dumping barge; (b) reflectance of TSS concentrations varied significantly when the TSS was under 10 mg/L.

References

- Cillero Castro, C.; Domínguez Gómez, J.A.; Delgado Martín, J.; Hinojo Sánchez, B.A.; Cereijo Arango, J.L.; Cheda Tuya, F.A.; Díaz-Varela, R. An UAV and Satellite Multispectral Data Approach to Monitor Water Quality in Small Reservoirs. *Remote Sens.* **2020**, *12*, 1514. [[CrossRef](#)]
- Klemas, V.V. Coastal and environmental remote sensing from unmanned aerial vehicles: An overview. *J. Coast. Res.* **2015**, *31*, 1260–1267. [[CrossRef](#)]
- Johansen, K.; Dunne, A.F.; Tu, Y.-H.; Almashharawi, S.; Jones, B.H.; McCabe, M.F. Dye tracing and concentration mapping in coastal waters using unmanned aerial vehicles. *Sci. Rep.* **2022**, *12*, 1141. [[CrossRef](#)] [[PubMed](#)]
- Finkbeiner, M.; Stevenson, B.; Seaman, R. *Guidance for Benthic Habitat Mapping: An Aerial Photographic Approach*; NOAA: Washington, DC, USA, 2001.
- Vize, S.; Coggan, R. *Review of Standards and Protocols for Seabed Habitat Mapping*; MESH 2.1; European Commission: Brussels, Belgium, 2005.

6. Duffy, J.P.; Cunliffe, A.M.; DeBell, L.; Sandbrook, C.; Wich, S.A.; Shutler, J.D.; Myers-Smith, I.H.; Varela, M.R.; Anderson, K. Location, location, location: Considerations when using lightweight drones in challenging environments. *Remote Sens. Ecol. Conserv.* **2018**, *4*, 7–19.
7. Ratcliffe, N.; Guihen, D.; Robst, J.; Crofts, S.; Stanworth, A.; Enderlein, P. A protocol for the aerial survey of penguin colonies using UAVs. *J. Unmanned Veh. Syst.* **2015**, *3*, 95–101. [[CrossRef](#)]
8. Doukari, M.; Batsaris, M.; Papakonstantinou, A.; Topouzelis, K. A protocol for aerial survey in coastal areas using UAS. *Remote Sens.* **2019**, *11*, 1913. [[CrossRef](#)]
9. Cheng, L.; Tan, X.; Yao, D.; Xu, W.; Wu, H.; Chen, Y. A Fishery Water Quality Monitoring and Prediction Evaluation System for Floating UAV Based on Time Series. *Sensors* **2021**, *21*, 4451. [[CrossRef](#)] [[PubMed](#)]
10. Koparan, C.; Koc, A.B.; Privette, C.V.; Sawyer, C.B. In situ water quality measurements using an unmanned aerial vehicle (UAV) system. *Water* **2018**, *10*, 264. [[CrossRef](#)]
11. Cheng, K.; Chan, S.N.; Lee, J.H. Remote sensing of coastal algal blooms using unmanned aerial vehicles (UAVs). *Mar. Pollut. Bull.* **2020**, *152*, 110889. [[CrossRef](#)] [[PubMed](#)]
12. McEliece, R.; Hinz, S.; Guarini, J.-M.; Coston-Guarini, J. Evaluation of Nearshore and Offshore Water Quality Assessment Using UAV Multispectral Imagery. *Remote Sens.* **2020**, *12*, 2258. [[CrossRef](#)]
13. Koparan, C. *UAV-Assisted Water Quality Monitoring*; Clemson University: Clemson, SC, USA, 2020.
14. DJI Matrice 600 Pro. Available online: <https://www.dji.com/sg/matrice600-pro> (accessed on 10 March 2022).
15. BaySpec Inc. OCITM-F Hyperspectral Imager (VIS-NIR, SWIR). Available online: <https://www.bayspec.com/spectroscopy/oci-f-hyperspectral-imager/> (accessed on 10 March 2022).
16. Turner, I.L.; Harley, M.D.; Drummond, C.D. UAVs for coastal surveying. *Coast. Eng.* **2016**, *114*, 19–24. [[CrossRef](#)]
17. Vélez-Nicolás, M.; García-López, S.; Barbero, L.; Ruiz-Ortiz, V.; Sánchez-Bellón, Á. Applications of unmanned aerial systems (UASs) in hydrology: A review. *Remote Sens.* **2021**, *13*, 1359. [[CrossRef](#)]
18. Kieu, H.T.; Law, A.W.-K. Remote sensing of coastal hydro-environment with portable unmanned aerial vehicles (pUAVs) a state-of-the-art review. *J. Hydro-Environ. Res.* **2021**, *37*, 32–45. [[CrossRef](#)]
19. Kwan, C.; Ayhan, B. Enhancing Safety of UAVs in National Airspace. In Proceedings of the 2019 IEEE 9th Annual Computing and Communication Workshop and Conference (CCWC), Las Vegas, NV, USA, 7–9 January 2019; pp. 617–622.
20. Koparan, C.; Koc, A.B.; Privette, C.V.; Sawyer, C.B.; Sharp, J.L. Evaluation of a UAV-Assisted Autonomous Water Sampling. *Water* **2018**, *10*, 655. [[CrossRef](#)]
21. Becker, R.H.; Sayers, M.; Dehm, D.; Shuchman, R.; Quintero, K.; Bosse, K.; Sawtell, R. Unmanned aerial system based spectroradiometer for monitoring harmful algal blooms: A new paradigm in water quality monitoring. *J. Great Lakes Res.* **2019**, *45*, 444–453. [[CrossRef](#)]
22. Bushnaq, O.M.; Kishk, M.A.; Celik, A.; Alouini, M.-S.; Al-Naffouri, T.Y. Optimal deployment of tethered drones for maximum cellular coverage in user clusters. *IEEE Trans. Wirel. Commun.* **2020**, *20*, 2092–2108. [[CrossRef](#)]
23. Kishk, M.A.; Bader, A.; Alouini, M.-S. On the 3-D placement of airborne base stations using tethered UAVs. *IEEE Trans. Commun.* **2020**, *68*, 5202–5215. [[CrossRef](#)]
24. Doukari, M.; Papakonstantinou, A.; Batsaris, M.; Topouzelis, K. Preview of a protocol for UAV data collection in coastal areas. In Proceedings of the Sixth International Conference on Remote Sensing and Geoinformation of the Environment (RSCy2018), Paphos, Cyprus, 26–29 March 2018; p. 1077314.
25. Doukari, M.; Batsaris, M.; Topouzelis, K. UASea: A Data Acquisition Toolbox for Improving Marine Habitat Mapping. *Drones* **2021**, *5*, 73. [[CrossRef](#)]
26. Liu, H.; Yu, T.; Hu, B.; Hou, X.; Zhang, Z.; Liu, X.; Liu, J.; Wang, X.; Zhong, J.; Tan, Z.; et al. UAV-Borne Hyperspectral Imaging Remote Sensing System Based on Acousto-Optic Tunable Filter for Water Quality Monitoring. *Remote Sens.* **2021**, *13*, 4069. [[CrossRef](#)]
27. Jaud, M.; Le Dantec, N.; Ammann, J.; Grandjean, P.; Constantin, D.; Akhtman, Y.; Barbieux, K.; Allemand, P.; Delacourt, C.; Merminod, B. Direct georeferencing of a pushbroom, lightweight hyperspectral system for mini-UAV applications. *Remote Sens.* **2018**, *10*, 204. [[CrossRef](#)]
28. DJI Ronin MX. Available online: <https://www.dji.com/sg/ronin-mx> (accessed on 10 March 2022).
29. DJI D-RTK GNSS. Available online: <https://www.dji.com/sg/d-rtk/info> (accessed on 10 March 2022).
30. OmniCharger Inc. Omni Mobile 25600. Available online: <https://www.omnicharge.co/products/omni-mobile-25600> (accessed on 10 March 2022).